Supplemental Data

Intraflagellar Transport Protein 27 Is a Small G Protein Involved in Cell-Cycle Control

Hongmin Qin, Zhaohui Wang, Dennis Diener, and Joel Rosenbaum

Supplemental Experimental Procedures

Identification of the IFT27 Gene

Peptide sequence of IFT27 was generated for identification of the gene encoding IFT27. For this end, the detergent soluble membrane plus matrix fraction of flagella was fractionated on a sucrose density gradient and fractions were subjected to SDS-PAGE. IFT27 was identified on these gels by its molecular weight and by cosedimentation with other IFT proteins at 16S (Figure S1). IFT27 was excised from the gel and subjected to internal peptide-sequence analysis [S1] yielding two micropeptide sequences: EVKPIDITATLR and DADAPFLSIATTFYR. These two peptide sequences were used for searching the GeneBank database and were matched to several *Chlamydomonas* EST sequences. A single predicted protein Chlre3:129193 from the website http://genome.jgi-psf.org/cgi-bin/dispGeneModel?db=Chlre3&id=129193 includes these two peptides and matches all the EST sequences. The predicted cDNA for Chlre3:129193 was confirmed by RT-PCR from total mRNA extracted from wild-type *Chlamydomonas* cells. A 1117 bp segment of IFT27 genomic DNA was generated by PCR from total *Chlamydomonas* DNA, and a comparison of this sequence to the IFT27 cDNA identified four introns and four exons (Figure S1) including a 615 bp open reading frame encoding IFT27. The protein is predicted to have a pI of 5.28 and a molecular weight of 23 kDa with the software described in [S2].

Antibodies

Three antigens were used for making the polyclonal antibodies against IFT27. One was a synthesized peptide MVKKEVKPIDI TATLRC, encompassing the N-terminal 17 amino acids of IFT27. The other two were proteins expressed in *E. coli* and purified. One was a full-length IFT27 with a maltose-binding protein (MBP) tag on its N terminus. The other was also a full-length IFT27 but was tagged with 6× His. MBP-IFT27 was purified soluble, whereas 6× His-IFT27 was purified in denatured form. Antibodies were made by subcutaneous injection of fusion proteins or peptide into rabbits by the Yale Biotechnology Services (New Haven, CT) (6× His-IFT27) or the Pocono Rabbit Farm and Laboratory (peptide and MBP-IFT27) to produce antisera. Antibodies produced against peptide, 6× His-IFT27, and MBP-IFT27 were affinity purified from synthesized peptide, 6× His-IFT27 fusion protein, or GST-IFT27 fusion protein bound to CNBr-activated beads, respectively. Fusion proteins were purified according to the manufacturers' protocols. All the affinity-purified antibodies gave similar results on western blots of samples from flagella. However, the antibodies produced against the MBP-IFT27 antigen were used for detecting IFT27 on western blots of whole-cell extracts because they gave the cleanest results.

Other antibodies used in this study include antibodies against GFP (clone 7.1 and 13.1; Roche Diagnostics, Basel, SWI), α-tubulin (clone B-5-1-2, ascites fluid; Sigma), and HSP70B (provided by Dr. C.F. Beck at Univ. of Freiburg) [S3]. IFT polypeptide antibodies included antibodies to *Chlamydomonas* IFT172, IFT57, IFT81, IFT139, FLA10 [S1], IFT74/72 [S4], and IFT46 [S5].

Nucleic-Acid Manipulations and Transformation

We used two approaches to achieve the desired RNAi knockdown of IFT27 expression. The first approach was essentially as previously described [S6]. In brief, genomic DNA that included the partial *IFT27* gene (1–1111 bp) and its native promoter (comprised of 1551 bp upstream sequence of the IFT27 gene) was obtained by PCR from total genomic DNA. A cDNA fragment of *IFT27* (1–570 bp) was obtained through RT-PCR. These two fragments were cloned into the TOPO-PCRII vector (Invitrogen). The cDNA fragment was cut out and inserted downstream of the genomic fragment in reverse orientation relative to the genomic piece. Finally, a PvuII fragment from plasmid pIS103 [S7] (provided by P. Hegemann at University of Berlin, Germany) containing the selectable marker *aphVIII* gene was ligated into the construct. This RNAi construct was called IFT27RNAi-1. A similar approach was used for generating the IFT52 RNAi construct. The second approach was a cosilencing method [S8]. A DNA fragment including the forward partial IFT27 genomic gene (1–291 bp) and the inverted piece (67–133 bp) were inserted into the Maa7/X IR vector [S8]. This RNAi construct was called IFT27RNAi-2. In all constructs, the newly formed junctions were subjected to sequencing. Information for the primers is available upon request.

For generating the IFT27::GFP construct, the full-length genomic DNA of *IFT27*, without its stop codon, including the 1.5 kb upstream promoter region (total 4 kb) was obtained through PCR from total genomic DNA. The full-length GFP fragment including the 230 bp downstream 3′UTR (total 1.0 kb) was obtained through PCR from a CrGFP plasmid [S9]. These two PCR products were mixed and used as the third PCR template for generating the chimeric IFT27::GFP gene driven by the IFT27 native promoter. This IFT27::GFP chimeric gene fragment was cloned into a TOPO PCRII vector. Subsequently, another fragment containing the selectable marker *aphVIII* gene was added into the same construct. In all constructs, all the fragments and the newly formed junctions were subjected to sequencing.

Wild-type CC125 cells were used for transformation. The cell wall was first removed by treatment with autolysin. The DNA was introduced into the cells by the glass-bead method [S10]. All the transformants except for IFT27RNAi-2 were selected on plates with 15 μg/ml paromomycin (Sigma). The culture conditions for selecting clones harboring the transgene IFT27RNAi-2 was in accordance with the method in [S8].

Supplemental References

S1. Cole, D.G., Diener, D.R., Himelblau, A.L., Beech, P.L., Fuster, J.C., and Rosenbaum, J.L. (1998). *Chlamydomonas* kinesin-II-dependent intraflagellar transport (IFT): IFT particles contain proteins required for ciliary assembly in *Caenorhabditis elegans* sensory neurons. J. Cell Biol. *141*, 993–1008.

S2. Wilkins, M.R., Gasteiger, E., Bairoch, A., Sanchez, J.C., Williams, K.L., Appel, R.D., and Hochstrasser, D.F. (1999). Protein identification and analysis tools in the ExPASy server. Methods Mol. Biol. *112*, 531–552.

S3. Drzymalla, C., Schroda, M., and Beck, C.F. (1996). Light-inducible gene HSP70B encodes a chloroplast-localized heat shock protein in *Chlamydomonas reinhardtii*. Plant Mol. Biol. *31*, 1185–1194.

S4. Qin, H., Diener, D.R., Geimer, S., Cole, D.G., and Rosenbaum, J.L. (2004). Intraflagellar transport (IFT) cargo: IFT transports flagellar precursors to the tip and turnover products to the cell body. J. Cell Biol. *164*, 255–266.

S5. Lucker, B.F., Behal, R.H., Qin, H., Siron, L.C., Taggart, W.D., Rosenbaum, J.L., and Cole, D.G. (2005). Characterization of the intraflagellar transport complex B core: Direct interaction of the IFT81 and IFT74/72 subunits. J. Biol. Chem. *280*, 27688–27696.

S6. Huang, K., and Beck, C.F. (2003). Phototropin is the blue-light receptor that controls multiple steps in the sexual life cycle of the green alga *Chlamydomonas reinhardtii*. Proc. Natl. Acad. Sci. USA *100*, 6269–6274.

S7. Sizova, I., Fuhrmann, M., and Hegemann, P. (2001). A Streptomyces rimosus aphVIII gene coding for a new type phosphotransferase provides stable antibiotic resistance to *Chlamydomonas reinhardtii*. Gene *277*, 221–229.

S8. Rohr, J., Sarkar, N., Balenger, S., Jeong, B.R., and Cerutti, H. (2004). Tandem inverted repeat system for selection of

effective transgenic RNAi strains in *Chlamydomonas*. Plant J. *40*, 611–621.

S9. Fuhrmann, M., Oertel, W., and Hegemann, P. (1999). A synthetic gene coding for the green fluorescent protein (GFP) is a versatile reporter in *Chlamydomonas reinhardtii*. Plant J. *19*, 353–361.

S10. Kindle, K.L. (1990). High-frequency nuclear transformation of *Chlamydomonas reinhardtii*. Proc. Natl. Acad. Sci. USA *87*, 1228–1232.

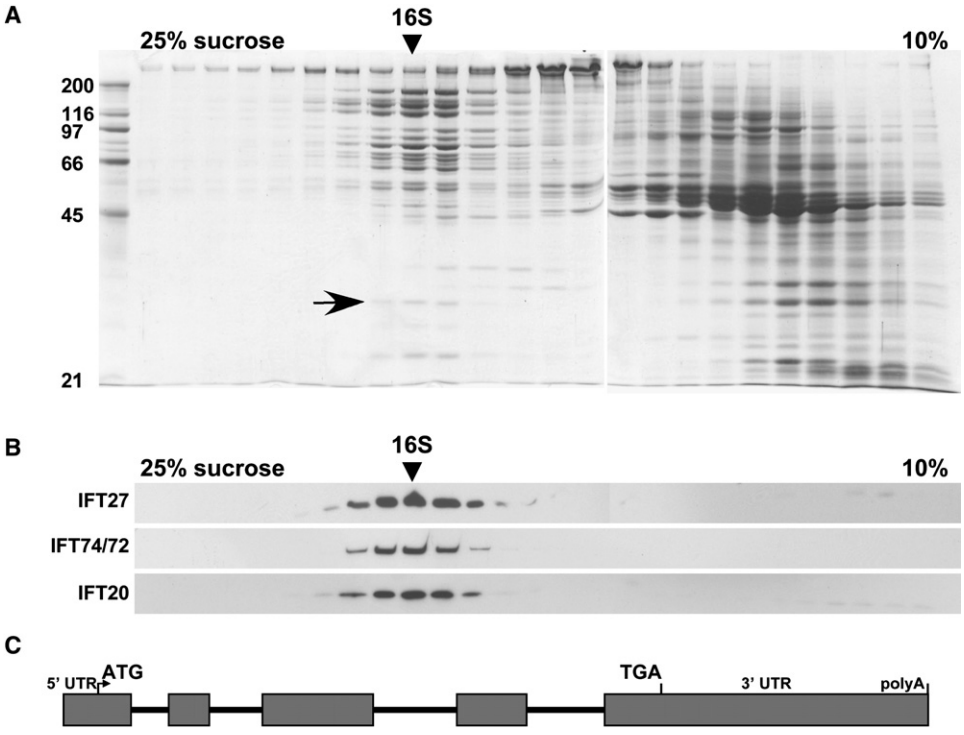

Figure S1. IFT27 Cosediments with Other IFT Particle Proteins at 16S on Sucrose Density Gradients

(A) Coomassie-blue-stained gels of the sucrose-density-gradient fractions of the wild-type flagellar membrane plus matrix. The 16S peak of IFT particle subunits is indicated by an arrowhead, and the IFT27 band is marked with an arrow.

(B) Immunoblots of similar gels probed for several IFT polypeptides. IFT27 cosediments with the other IFT proteins at 16S.

(C) Schematic representation of the IFT27 gene (1.7 kb) with five exons (boxes) that make up the 615 bp cDNA.

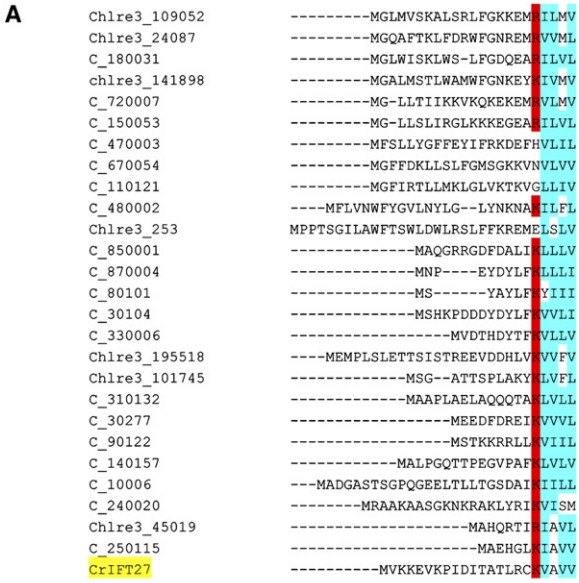

Figure S2. The First Exon of IFT27 Has Limited Similarity to Other Small GTPases in *Chlamydomonas*

(A) The predicted protein sequences of 27 small GTPases were found in the *Chlamydomonas* genomic database and were aligned by Clustal ×1.81 software. Shown here is the region corresponding to the first exon of IFT27, which exhibits very limited similarity among these genes and throughout the Ras superfamily except for the last five amino acids (highlighted red represents positive charge; cyan, aliphatic).

(B) Dendrogram of *Chlamydomonas* small GTPases was generated with software Philip 3.64. (IFT27 is highlighted in yellow as "CrIFT27.")

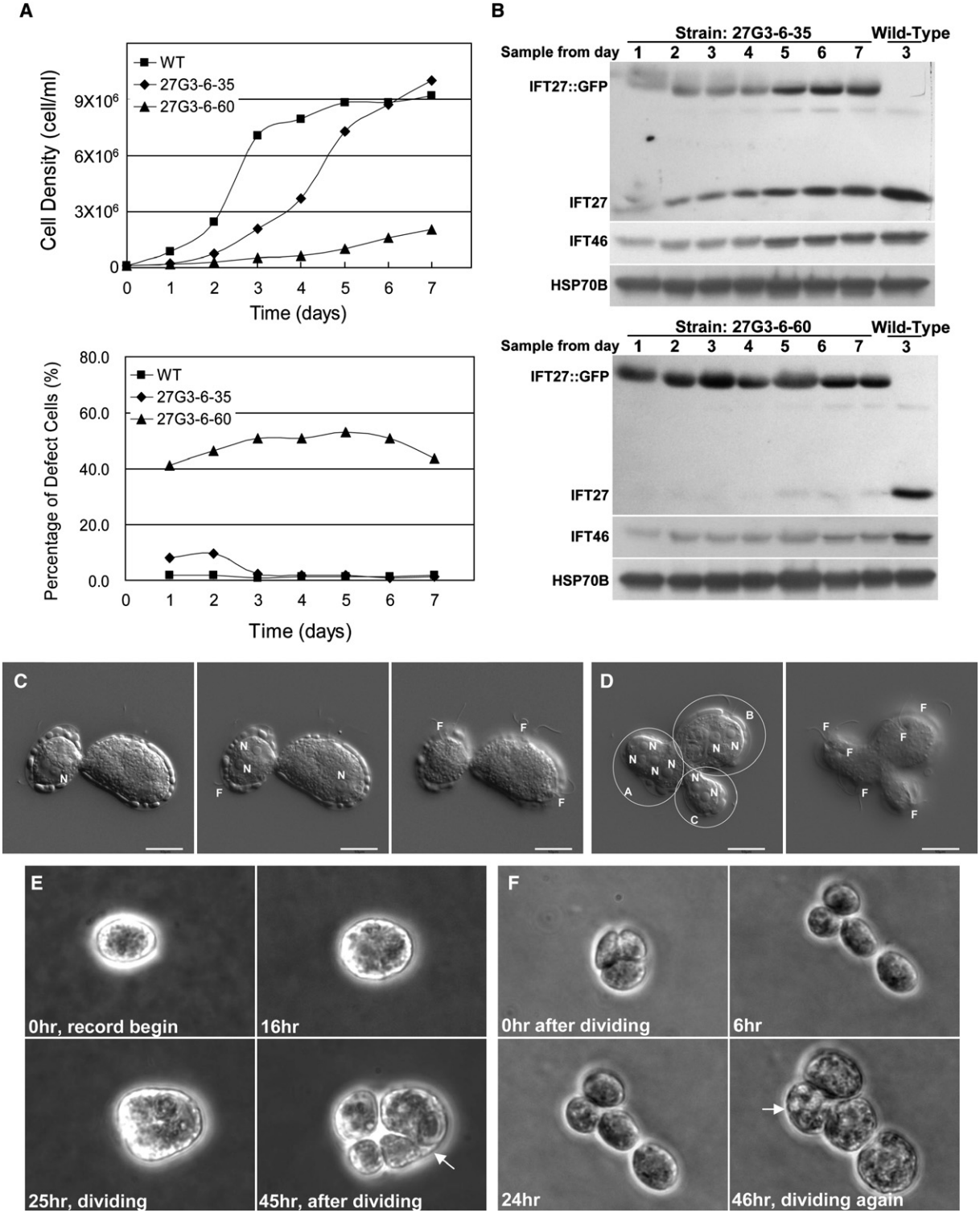

Figure S3. Native IFT27 Correlates with Dividing Defects in Clones Expressing a High Level of IFT27::GFP

Several GFP-tagged clones showed defects similar to the IFT27 RNAi cells. Two subclones of one such strain (27G3-6) are shown.

(A) Growth curves and counts of defective cells (multiple sets of flagella or nuclei) were plotted for two subclones, 27G3-6-35 and 27G3-6-60. 27G3-6-60 grew very slowly and had 40%–50% defective cells, whereas 27G3-6-35 had a weaker phenotype. The percentage of defective 27G3-6-35 cells during the first 2 days was approximately 10% compared to ~1% in the wild-type. Cells were cultured in TAP medium under the same conditions as in Figure 4.

(B) Immunoblots of 27G3-6-35 and 27G3-6-60 showing the level of IFT27, IFT27::GFP, and IFT46 and showing the HSP70B as a loading control. Expression of IFT27 partially recovered in 27G3-6-35 concomitant with an increase in the growth rate and the disappearance of abnormal cells. Restoration of the wild-type phenotype in these cells demonstrates the defects were not caused by disruption of a key gene by transformation. Expression of native IFT27 remained low in 27G3-6-60, and cells showed severe defects throughout the time course. The high level of IFT27::GFP

in this subclone indicates that the reduction of native IFT27 is not due to an unintentional RNAi effect and that with GFP attached to its C terminus, IFT27 can not fulfill its role in cell division. However, in the flagella IFT27::GFP moves by IFT (Figure 3B), sediments with IFT complexes (Figure 2B), and prevents the disappearance of IFT46 (shown) and other IFT proteins (data not shown).

(C and D) DIC images of two 27G3-6 cells. Images were taken under the same conditions as Figure 4C. Scale bars are represent 10 μm.

(C) Three focal planes showing asymmetric division in a monster-like cell. Three nuclei "N" and two pairs of flagella "F" were distributed into the left part of the cell, whereas the right part contained only one nucleus and two pairs of flagella.

(D) Two focal planes of a monster-like cell showing uncoupling of nuclear and flagellar duplication. Eight nuclei and six pairs of flagella were found in the three parts of this cell: A = 4N + 3F; B = 2N + 2F; C = 2N + 1F.

(E and F) 27G3-6 cells have an elongated cell cycle. Cells were embedded in 0.5% low-melt agarose in TAP media, grown under continuous light, and photographed periodically using phase microscopy. (E) This cell began division approximately 25 hr after it was first recorded. Division was asymmetric and was not completed 20 hr after division began (45 hr, indicated by the arrow). (F) This cell was recorded from just after division to the beginning of next division (46 hr, indicated by the arrow), illustrating a cell-cycle duration of approximately 2 days. The cycle time for wild-type cells under the same conditions was 12–14 hr (data not shown). In more than 90% of the cells, the cycle time was approximately 2–3 days and division itself lasted much longer (>6 hr) than in wild-type cells (~2 hr) (data not shown).

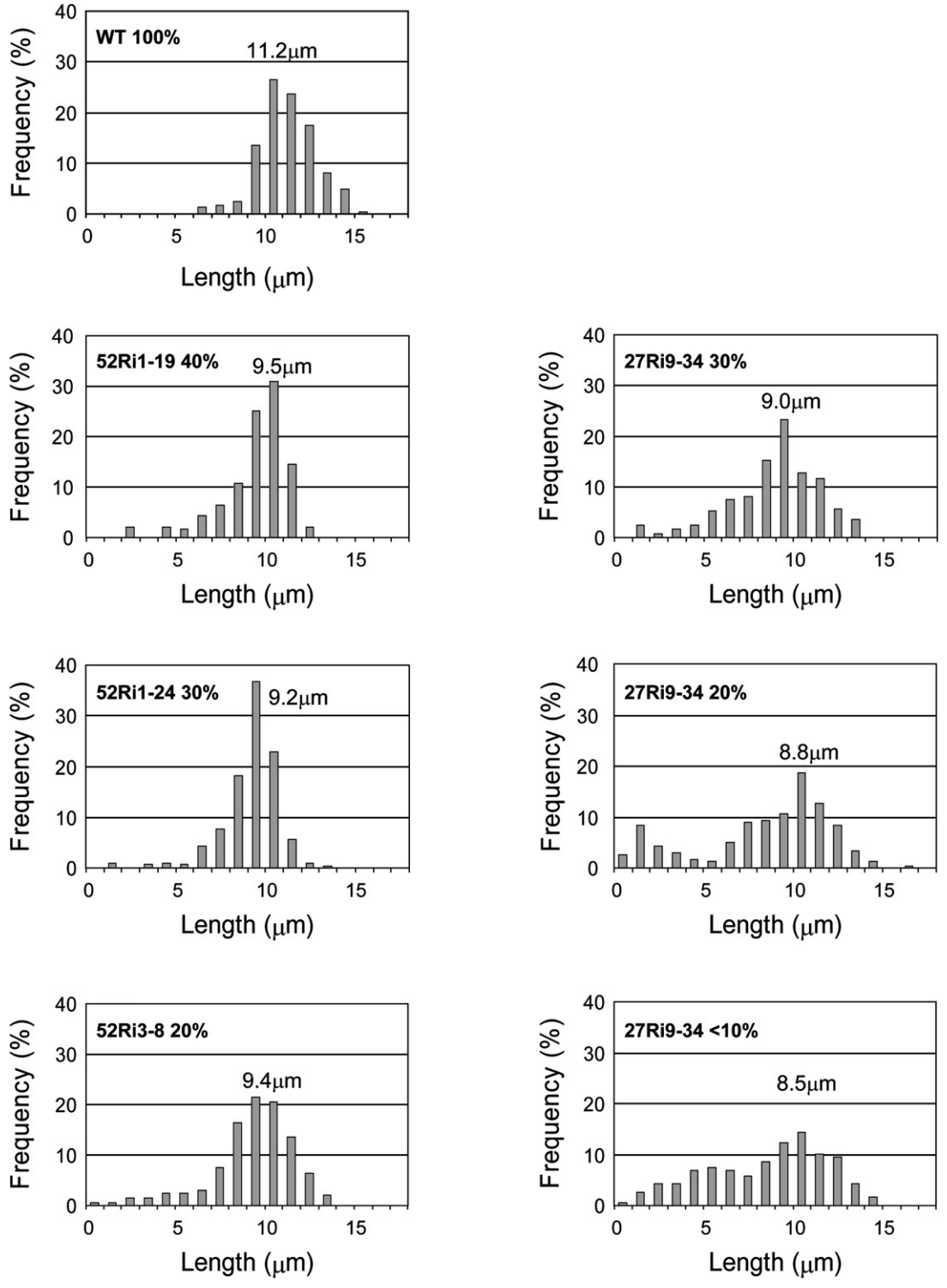

Figure S4. Histograms of Flagellar Lengths from Wild-Type Cells and from IFT52 and IFT27 Knockdown Cells

The approximate percentage of IFT27 and IFT52 remaining in the cells is listed as is the mean flagellar lengths.